Combining Orbital and Proximal Sensing to Map Management Zones in Precision Viticulture: A Spatiotemporal Analysis

Eduardo Antonio Speranza[1], José Renan da Silva e Silva[2], Leonardo Ruan de Souza Correa[2], Luis Henrique Bassoi[3]

1 Brazilian Agricultural Research Corporation (Embrapa Digital Agriculture), Campinas, SP, Brazil.

2 São Paulo State University (UNESP), College of Agricultural Sciences, Botucatu, SP, Brazil.

3 Brazilian Agricultural Research Corporation (Embrapa Instrumentation), São Carlos, SP, Brazil.

A paper from the Proceedings of the

17th International Conference on Precision Agriculture and 11th Brazilian Congress on Precision and Digital Agriculture

13-15 July 2026

Porto Alegre, Brazil

Abstract.

The practice of precision viticulture enables mapping of spatial and temporal variability of internal vineyard factors. Because grapevines are perennial crops, they exhibit consistent behavior across crop cycles, requiring an analysis of the interdependence between causes and effects over time, as well as between quality and yield. Edaphoclimatic conditions and vineyard management directly influence grape ripening and oenological characteristics. Vegetative vigor, observed through non-uniform patterns, highlights differences in the environmental conditions inherent to each growing area. To characterize this variability, proximal remote sensing which provides detailed, fine-scale canopy measurements and modern high-resolution orbital sensors have emerged as promising tools. The integration of these approaches represents a significant frontier for delineating management zones (MZs). Therefore, the objective of this study was to evaluate and compare the use of high-resolution proximal and orbital remote sensing for the delineation of MZs. The research was conducted in Espírito Santo do Pinhal, São Paulo State, Brazil. Commercial vineyards were evaluated comprising three wine grape cultivars (Cabernet Franc, Cabernet Sauvignon, and Chardonnay) managed under a winter harvest system over two consecutive crop cycles (2018 and 2019). Vegetation indices (NDVI, RVI, and SAVI) were acquired proximally via an active optical sensor and orbitally via PlanetScope nanosatellites during the berry ripening stage. Overall results demonstrated that both data sources successfully and consistently delineated statistically distinct MZs (high and low vigor), providing highly complementary between them. Orbital imagery provides a reliable macro-level overview for spatial planning, whereas proximal data refines boundaries and details internal variability, enabling more precise and efficient vineyard management.

Keywords.

Vegetation Indices; winter wine; geostatistics; clustering analysis.

The authors are solely responsible for the content of this paper, which is not a refereed publication. Citation of this work should state that it is from the Proceedings of the 17th International Conference on Precision Agriculture and 11th Brazilian Congress on Precision and Digital Agriculture. EXAMPLE: Last Name, A. B. & Coauthor, C. D. (2026). Title of paper. In Proceedings of the 17th International Conference on Precision Agriculture and 11th Brazilian Congress on Precision and Digital Agriculture (unpaginated, online). Monticello, IL: International Society of Precision Agriculture and Brazilian Congress on Precision and Digital Agriculture.

Introduction

The practice of precision viticulture enables the mapping of the spatial and temporal variability of internal vineyard factors, with a particular focus on the temporal dimension since it is a perennial crop, unlike occurs in annual crops (Costa, 2021). Grapevines exhibit consistent behavior from one crop cycle to the next, requiring an analysis of the interdependence between causes and effects over time, as well as between quality and yield. Edaphoclimatic conditions and vineyard management directly influence grape ripening and their oenological characteristics (Costa, 2021), making the characterization of internal spatial variability essential for decision-making.

The vegetative vigor of grapevines, observed through its non-uniform patterns, highlights differences in the environmental conditions inherent to each growing area. In precision viticulture, inferences about the vegetative development status are made by estimating vegetation indices derived from canopy reflectance (ρ) (Costa, 2021). Studies validate that proximal and remote sensors allow for the delineation of management zones based on vegetative vigor, water status, and microclimate (Matese et al., 2019; Urretavizcaya et al., 2016).

Proximal remote sensing is characterized by data acquisition in close proximity to the target of interest, allowing for detailed and specific measurements, including the identification of variations in leaf chemical composition, chlorophyll content, and plant physiological status (Homolová et al., 2013). Concurrently, there has been a notable improvement in the quality of orbital sensors. High spatial resolution nanosatellites have emerged as promising tools for mapping vegetative vigor at an agricultural scale (Engesat, 2019). The PlanetScope® constellation operates in a sun-synchronous orbit with daily revisit capabilities, a spatial resolution of 3 m per pixel, and spectral bands in the visible and infrared spectra, providing images with high-quality radiometric and geometric processing (Planet Labs, 2023).

The integration of proximal and orbital approaches represents a significant frontier for precision viticulture, particularly for the delineation of management zones in vineyards. The objective of this study was to evaluate and compare high-resolution proximal and orbital remote sensing for delineating management zones over two consecutive crop cycles of three grapevines cultivars harvested in winter (enabled by double pruning practice for winter wine production) in Southeast Brazil.

Materials and Methods

Study Area

The study was conducted at a winery located in Espírito Santo do Pinhal, São Paulo State, Brazil (22° 11’ 27’’ S; 46° 44’27’’). Four commercial vineyards comprising three cultivars were evaluated: A1 (1.50 ha), with cv. Cabernet Franc; A2 (0.97 ha), with cv. Cabernet Sauvignon; and areas A3 and A4 (0.60 and 0.50 ha, respectively), with cv. Chardonnay. Elevations in these areas range from 875 to 1200 m. The climate, according to the Köppen classification, is Cwa (humid subtropical, with dry winters and hot summers) (Alvares et al., 2013).

Grapevines were trained in a vertical shoot positioning (VSP) system with a row spacing of 2.5 and 3.0 m and 1.0 m between plants. The areas feature clay-textured soils (Cambisols and Regosols) and are managed under drip irrigation. The crop cycles evaluated were 2018 and 2019, with data collection performed during the berry ripening phenological stage (BBCH 81–89), according to Lorenz et al. (1995).

Proximal sensing

Grapevine canopy reflectance (ρ, dimensionless) was measured using a Crop Circle ACS-430 active optical sensor (Holland Scientific Inc., Lincoln, NE, USA) paired with a GeoSCOUT® GLS-400 datalogger (Holland Scientific Inc., Lincoln, NE, USA). The sensor measures ρ at three wavelengths (λ): 670 nm (ρRED), 730 nm (ρRE) and 780 nm (ρNIR), with an acquisition rate of 10 readings per second during walking surveys along the plant rows. The measurements were georeferenced using HiPer® GGD GNSS receivers (Topcon, Pleasanton, CA, USA), operating in RTK or autonomous mode with sub-metric accuracy.

In the Cabernet Franc and Cabernet Sauvignon areas (A1 and A2), data collection generated approximately 20,000 points; and in the Chardonnay areas (A3 and A4), it generated approximately 15,000 and 12,000 points, respectively (Oldoni, 2019; Silva, 2020). All field data collection occurred during the berry ripening phenological stage.

Orbital sensing

Orbital imagery was acquired from PlanetScope® nanosatellites (Planet Labs, San Francisco, CA, USA) via RedeMAIS/MJSP as Analytic Ortho Scenes (Level 3B). These products feature a 3 m spatial resolution, four spectral bands (Blue, Green, Red, and Near-Infrared), and 12-bit radiometric resolution. The scenes underwent radiometric and atmospheric corrections, as well as orthorectification, ensuring a geometric accuracy of less than 10 m (RMSE at the 90th percentile) (Planet Labs, 2023).

Images were selected to closely align with the dates of the proximal sensing (during the berry ripening stage), prioritizing scenes with less than 10% cloud cover. Band processing and the calculation of vegetation indices were performed using QGIS software (v.3.34.9). Based on the spectral compatibility between the ACS-430 and PlanetScope sensors, the Red and NIR bands were used to calculate the Normalized Difference Vegetation Index (NDVI) (Rouse et al., 1974), the Ratio Vegetation Index (RVI) (Jordan, 1969), and the Soil Adjusted Vegetation Index (SAVI) (Huete, 1988) using an adjustment factor (L) of 0.5 for all evaluated cultivars.

Spatial standardization and geostatistics

To ensure spatial compatibility between the proximal data and the 3 m grid of the PlanetScope imagery, specific procedures were applied based on the sample size. Given the dataset of over 12,000 points per area, local kriging was performed using Vesper 1.62 software (Minasny, McBratney, & Whelan, 2005). Geometric compatibility was verified through the visual overlay of the imagery and the georeferenced points.

Potential management zones delineation and statistical analysis

Management zones were delineated using the unsupervised K-means clustering algorithm in R software (v. 4.4.1). After removing sampling points with missing data in either year, the vegetation indices (NDVI, RVI, and SAVI) were standardized using the Z-score method to account for scale variations. To ensure temporally consistent patterns across the 2018 and 2019 cycles, all six variables (three indices per year) were used simultaneously as inputs for the clustering analysis.

The number of potential management zones was set to k = 2 to distinguish between high (Zone 1) and low (Zone 2) vegetative vigor. The algorithm was executed with 25 random initializations to minimize the within-cluster sum of squares. Clustering quality was validated using the average silhouette width (Rousseeuw, 1987), and group separation was visualized via Principal Component Analysis (PCA). Final spatial mapping of the management zones was performed in QGIS.

Results and Discussion

Descriptive statistics of reflectances and vegetation indices

Results revealed systematic differences between the proximal and orbital sensors. The proximal sensor recorded higher NIR (36–37%) and lower Red (4–5%) reflectances, whereas the orbital sensor exhibited lower NIR (30–35%) and higher Red (7–10%). Consequently, proximal vegetation indices were systematically higher; for instance, proximal NDVI ranged from 0.78 to 0.88, compared to 0.50 to 0.66 for the orbital NDVI, with RVI further amplifying this gap. SAVI exhibited expected inconsistencies between platforms due to variations in the soil adjustment factor (L) across different areas. These widely known discrepancies are primarily attributed to differences in spectral band specifications, viewing angles, atmospheric interference, and mixed pixels (canopy, soil, and shadow). Given the stronger soil background influence on orbital data, the inclusion of SAVI was essential to ensure a more robust analysis.

Defining the number of clusters and delineating management zones

The definition of the optimal number of clusters (k) yielded consistent results across sensors, cultivars, and crop cycles. The average silhouette width identified k = 2 as the optimal configuration for all evaluated plots, demonstrating excellent cluster separation and rendering initial a priori fixation unnecessary. Principal Component Analysis (PCA) corroborated this choice, as the first two principal components explained between 74% and 95% of the total variance, showing clear cluster separation for both proximal and orbital sensors. When testing k = 3, the variance explained by PC1 and PC2 remained above 90% for orbital data, whereas proximal data began revealing small pockets of local heterogeneity. For k ≥ 4, complete dissimilarity emerged between proximal and orbital datasets, precluding direct comparisons between platforms, consistent with findings by Correa (2025).

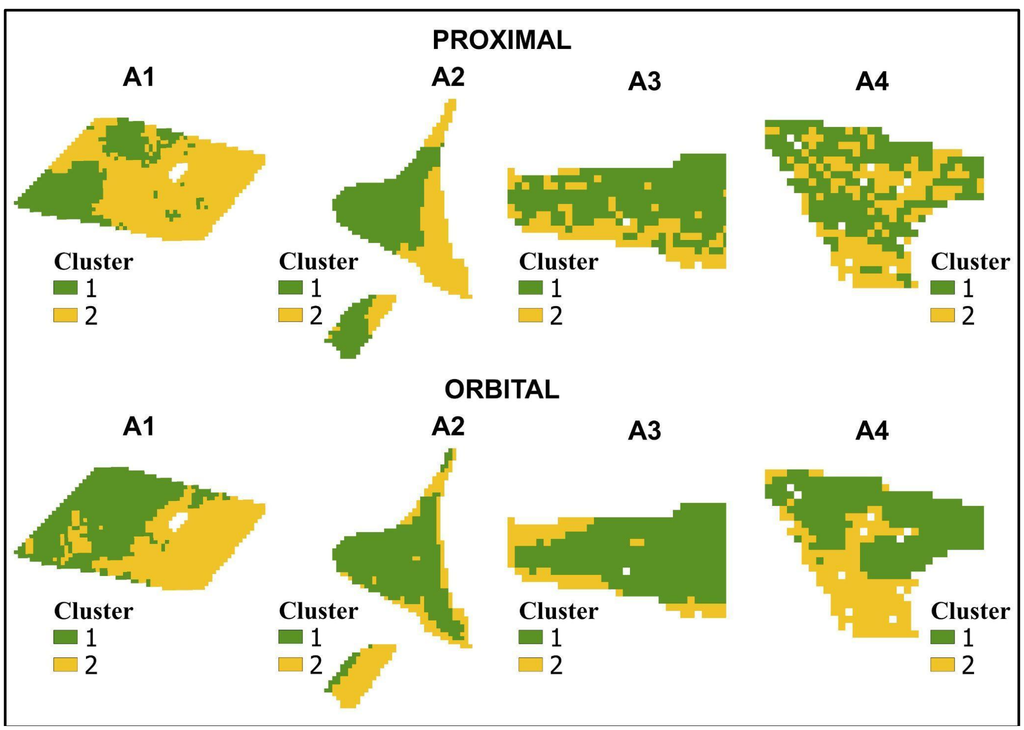

Figure 1. Maps of the management zones generated for the four areas. The upper panels display the proximal sensor data for the 2018 and 2019 cycles, while the lower panels show the orbital sensor data for the same years. Cluster 1 represents areas of higher vegetative vigor, and Cluster 2 represents areas of lower vegetative vigor.

Results indicate that orbital sensors offer greater stability and consistency in cluster separation, particularly in larger areas, whereas high-resolution proximal sensors better capture internal vineyard variability. However, in highly heterogeneous areas like A4, proximal data tends to introduce noise and excessive fragmentation, hindering agronomic interpretation. In such cases, the orbital sensor smoothed high-spatial-frequency fluctuations, yielding management zones with clearer boundaries and greater applicability for site-specific management (Figure 1).

Therefore, integrating both approaches is strategic: orbital sensors provide a reliable macro-level overview for planning, while proximal data refines boundaries, corroborating Hossain et al. (2025) regarding the benefits of sensor fusion for management zone delineation. Nonetheless, the 3 m PlanetScope resolution resulted in mixed pixels incorporating inter-row bare soil. For future research, sub-metric imagery, potentially acquired via Unmanned Aerial Vehicles (UAVs), is recommended to enhance target pixel filtering (Silva & Silva, 2026).

Clusterings statistical validation

The Kruskal-Wallis tests (χ^2) confirmed statistically significant differences between the two delineated management zones across all evaluated indices, sensors, and areas ($p < 0,001$), indicating that the K-means algorithm produced clusters with consistent spectral separation. Normality was rejected in all cases by the Shapiro-Wilk test, which justified the use of the non-parametric test as a substitute for a parametric ANOVA. In vineyard A1, χ^2 values ranged from 404.53 to 750.09 for the proximal indices and from 667.68 to 731.70 for the orbital ones. In vineyard A2, values ranged between 386.09 and 522.08 (proximal) and between 396.55 and 481.86 (orbital). In vineyards A3 and A4, which have smaller sample sizes, the χ^2 values were equally substantial: from 197.85 to 211.80 and from 125.49 to 180.15 for the proximal and orbital data of A3, respectively; and from 27.62 to 239.04 and from 181.08 to 185.61 for the proximal and orbital data of A4. The wider range observed in the proximal indices of A4 (χ^2 from 27.62 for RVI 2019 to 239.04 for SAVI 2018) reflects a temporally asymmetric separation between the two years in this area, with a more pronounced distinction in the 2018 indices.

Comparison between proximal and orbital sensing

Principal Component Analysis (PCA) confirmed a clear and significant separation between the two management zones across all areas and sensors (Table 1). The first two principal components (PC1 and PC2) explained over 93% of the total variance in all scenarios, indicating a primarily two-dimensional data structure. The Kruskal-Wallis test on PC1 scores was highly significant ($p < 0,001$) across the board. Orbital sensors tended to concentrate more variance in PC1 and PC2 combined (often > 99%) compared to proximal sensors. A notable exception occurred in the A4 proximal dataset, where variance was nearly evenly distributed between PC1 (47.96%) and PC2 (45.53%), with both components contributing significantly to zone separation ($\chi^2 = 52,49$; $p < 0,001$). Overall, both platforms yielded substantial effect sizes (Cohen's d > 2.0) for PC1, demonstrating comparable efficacy and reinforcing the consistency of both acquisition systems in delineating management zones.

Table 1. Principal Component Analysis of management zones by area and sensor (orbital and proximal sensing), with management zones separation evaluated by Kruskal-Wallis tests over component scores.

Area	Sensor	N	Z1	Z2	PC1 (%)	PC2 (%)	PC1+PC2 (%)	PC1 Z1	PC1 Z2	Cohen d	χ^2 PC1	χ^2 PC2
A1	Orbital	1300	645	655	67.92	31.83	99.75	-1.7385	1.7120	**3.295**	974.18	1.66
	Proximal	1300	415	885	68.31	27.21	95.52	-2.3387	1.0967	2.742	838.13	**68.77***
A2	Orbital	809	534	275	82.22	16.26	98.48	-1.2926	2.5100	**2.863**	543.89	0.01
	Proximal	809	485	324	82.43	12.93	95.35	-1.5191	2.2740	**3.059**	581.93	3.01
A3	Orbital	444	332	112	58.29	41.44	99.73	-0.8876	2.6311	**2.952**	249.79	1.48
	Proximal	444	292	152	64.02	30.84	94.86	1.1633	-2.2348	**2.939**	299.11	0.10
A4	Orbital	402	241	161	67.54	32.14	99.68	1.3364	-2.0004	**2.859**	288.84	0.22
	Proximal	402	231	171	47.96	45.53	93.49	-1.0518	1.4209	2.054	231.53	**52.49***

*Notes: Z1 = Zone 1 (greater vigor); Z2 = Zone 2 (less vigor). PC1% e PC2% = variance explained by first principal components. PC1 Zone 1 and PC2 Zone 2 = mean score of PC1 by zone (standardized data by Z-score). d = Cohen's d (effect separation size in PC1). χ^2 PC1 e χ^2 PC2 = Kruskal-Wallis statistics over component scores (all values of χ^2 PC1 with $p < 0,001$; * indicating χ^2 PC2 with $p < 0,05$).*

Conclusion

Both proximal and orbital sensors proved highly effective in delineating consistent and statistically distinct management zones (MZs) across all evaluated vineyards. Despite differences in index magnitudes, with proximal sensors capturing higher absolute values and fine-scale internal variability, and orbital sensors offering broader spatial integration, both data sources successfully discriminated vigor patterns.

In practice, these sensing platforms are highly complementary. Orbital imagery provides frequent monitoring and mapping of macro-level patterns over large areas, whereas proximal sensing refines the detection of fine-scale canopy variability and aids in map calibration. Therefore, an integrated workflow is recommended, combining orbital mapping for initial MZ delineation, proximal sampling for data harmonization, and agronomic validation using yield and grape quality metrics. Future studies should address the impact of mixed pixels in orbital imagery to further optimize the definition of management zones.

Acknowledgments

The authors thank Vinicola Guaspari for their support in conducting the experiments. This study was financed in part by the Coordenação de Aperfeiçoamento de Pessoal de Nível Superior - Brasil (CAPES) - Finance Code 001. The authors also acknowledge the Graduate Program in Agricultural Engineering at UNESP/FCA and Embrapa Instrumentation.

References

Alvares, C.A. et al. (2013) Köppen's climate classification map for Brazil. Meteorologische Zeitschrift 22:711–728.

Correa, L.R.S. (2025). Uso de sensores orbital e terrestre na delimitação de zonas de manejo em vitivinicultura de precisão. Master's dissertation, Faculdade de Ciências Agronômicas, Universidade Estadual Paulista (UNESP), Botucatu.

Costa, B.R.S. (2021). Zonas de vigor vegetativo para colheita seletiva em viticultura irrigada com base em sensoriamento proximal. PhD thesis, Faculdade de Ciências Agronômicas, Universidade Estadual Paulista (UNESP), Botucatu.

Engesat (2019). PlanetScope satellite imagery. http://www.engesat.com.br/imagem-de-satelite/planetscope/. Accessed Jan 2024.

Homolová, L. et al. (2013). Review of optical-based remote sensing for plant trait mapping. Ecological Complexity 15:1–16.

Hossain, M.T., Donat, M., Tougma, I.A., Bellingrath-Kimura, S.D., Grahmann K. (2025). Nitrogen-based proximal sensing and data fusion for management zone delineation. Agricultural & Environmental Letters 10(1):e70051. https://doi.org/10.1002/agg2.70051.

Huete, A. R. (1988). A soil-adjusted vegetation index (SAVI). Remote Sensing of Environment 25:295–309.

Jiang, Z. et al. (2008). Development of a two-band enhanced vegetation index without a blue band. Remote Sensing of Environment 112:3833–3845,

Jordan, C.F. (1969). Derivation of leaf-area index from quality of light on the forest floor. Ecology 50(4):663–666.

Kasimati, A. et al. (2023). Investigation of the similarities between NDVI maps from different proximal and remote sensing platforms in explaining vineyard variability. Precision Agriculture 24:1220–1240.

Macqueen, J. (1967). Some methods for classification and analysis of multivariate observations. In: Proceedings of the 5th Berkeley Symposium on Mathematical Statistics and Probability. University of California Press, Berkeley, pp 281–297.

Matese, A. et al (2019). Accurate in-field estimation of grapevine condition by integrating proximal and remote sensing. Remote Sensing 11(17):2009.

Minasny, B., McBratney, A.B., Whelan, B.M. (2005). Vesper version 1.62. Australian Centre for Precision Agriculture, Sydney.

Oldoni, H. (2019). Índice de vegetação por diferença normalizada de uma videira cv. Chardonnay. Master's dissertation, Faculdade de Ciências Agronômicas, Universidade Estadual Paulista (UNESP), Botucatu.

Planet Labs (2023). PlanetScope product specification. Planet Labs PBC, San Francisco. https://developers.planet.com/. Accessed Jan 2024.

Rouse, J.W. et al. (1974). Monitoring vegetation systems in the Great Plains with ERTS. In: Proceedings of the 3rd Earth Resources Technology Satellite-1 Symposium. NASA, Washington, pp 309–317.

Rousseeuw, P.J. (1987). Silhouettes: a graphical aid to the interpretation and validation of cluster analysis. Journal of Computational and Applied Mathematics 20:53–65.

Silva J.C., Oliveira P.M. (2019). Estrutura de dossel e saturação de índices de vegetação: comparativo proximal e orbital. Ciência Rural 49(12):1–8.

Silva & Silva, J.R. (2026). Comparação na delimitação de zonas de manejo por sensor proximal e orbital em vitivinicultura de inverno. Master's dissertation, Faculdade de Ciências Agronômicas, Universidade Estadual Paulista (UNESP), Botucatu.

Urretavizcaya, P. et al. (2016). Real-time sensor-based irrigation management. Precision Agriculture 17(4):745–757.